

Improved Meandered Gysel Combiner/Divider Design with Stepped-Impedance Load Line for High-Power Applications

Mehrdad Gholami^{1, *}, Rony E. Amaya², and Mustapha C. E. Yagoub¹

Abstract—This paper presents an improved structure of a Gysel combiner/divider suitable for high-power applications. The proposed structure makes use of stepped-impedance load line features to implement a simple, compact, low loss and sufficiently wideband Gysel configuration. It also improves isolation and facilitates design flexibility for the load location. Measurements agree with expected simulated results thus, demonstrating the proposed structure with a 10% fractional bandwidth while maintaining 20 dB of return loss and 0.25 dB of insertion loss.

1. INTRODUCTION

Among existing power combiners/dividers (PCDs), in-phase PCDs, such as Wilkinson, exhibit negligible unbalance amplitude over a wide bandwidth. This feature makes them good candidates for high-power applications since very small fractions of unbalance power between PCD ports could significantly degrade the operation of high-power devices like Solid State Power Amplifiers (SSPAs). Microstrip Wilkinson PCD can provide low Insertion Loss as well as High Isolation and Return Loss over acceptable bandwidths [1], while also exhibiting the most compact configuration over other PCDs. However, in most cases, the load resistor is too close to the body of the structure, resulting in Wilkinson PCDs that are prone to unwanted radiations from adjacent resistors, leading to a drastic reduction in their performance [2]. High-power RF resistors are still large in size although RF components providers are implementing smaller high-power RF devices. Thus implementing Wilkinson PCDs with high power resistors on a Printed Circuit Board (PCB) remains a challenge. One way to include high power RF resistor with minimum unwanted radiations would be to add a half-wavelength impedance sections to each arm and also between the load resistor ends and the Wilkinson's arms [3] (Fig. 1(a)). However, this scheme will obviously increase the size and severely degrade the total insertion loss.

During the last few years, several improvements have been made on Wilkinson PCD design but most of them are not still able to address these drawbacks [4–6].

In 1975, Gysel proposed a suitable configuration for high-power in-phase PCDs [7]. In this structure, two load resistors have been used outside of the structure body so large size resistors can be used with minimum concern about unwanted radiations. Note that this structure is still an in-phase PCD but if one of the loads is removed, the remaining configuration would be close to a rat race structure. The main drawback of the Gysel structure is that it is relatively bulkier (Fig. 1(b)). From there, many modifications to the original configuration have been suggested [8–15]. The measurement results of the referred works are summarized in Table 1.

In this paper, an enhanced Gysel PCD configuration is presented by inserting meandered stepped-impedance load lines to a conventional configuration, where the 50 Ω load resistors are directly connected to the Gysel PCD ring. This aims to add three additional degrees of freedom to the structure compared

Received 29 October 2016, Accepted 1 December 2016, Scheduled 10 December 2016

* Corresponding author: Mehrdad Gholami (mehrdad.gholami@uottawa.ca).

¹ School of Electrical Engineering and Computer Science, University of Ottawa, 800 King Edward Ave., Ottawa, ON, K1N 6N5, Canada. ² Department of Electronics, Carleton University, 1125 Colonel By Dr., Ottawa, ON, K1S 5B6, Canada.

to standard ones, leading to low insertion loss and high return loss over a wider bandwidth, as well as facilitating design flexibility for the load location. To understand the theory of operation, an even-odd mode analysis was used while all the design steps are refined by using commercial circuit/EM simulators such as Keysight ADS Momentum [16]. Analysis of the proposed PCD based on even-odd impedance model along with a step by step procedure is presented in Section 2. A design flow-chart of the proposed structure design is also presented to facilitate frequency scaling of the proposed design approach. To demonstrate the capabilities and scalability of the proposed PCD, three modified Gysel PCDs were designed and fabricated in different frequency bands and/or substrates. For each case, the measured results are successfully compared with the simulation ones as detailed in Section 3.

Table 1. Comparisons between measurement results of the reported Gysel structure.

Bandwidth (GHz) for	[8]	[10]	[11]	[12]	[13]	[14]	[15]
< 0.25 dB IL	0	0	0	0	0	0	1.6–2.2
< 0.5 dB IL	0	0	0	0	0	2.9–3.3	1.5–2.4
> 20 dB RL of port 1	4.5–7.7	1.3–1.7 & 2.3–2.7	Not presented	1–1.4 & 1.6–1.9	0.8–1.2	2.8–3.3	1.9–2.4
> 15 dB RL of port 2 or 3	5–7.6	1.3–2.6	Not presented	1.1–1.9	Not presented	2.9–3.2	1.7–2.5
> 15 dB IS	4–8.2	0–5	0.9–2.3	1.1–2	0.4–1.6	2.6–3.3	1.5–2.3
< 0.1 dB unbalance power between splitting ports	0	2.7–2.9	0.5–2.3	Not presented	Not presented	0	1.5–2.6

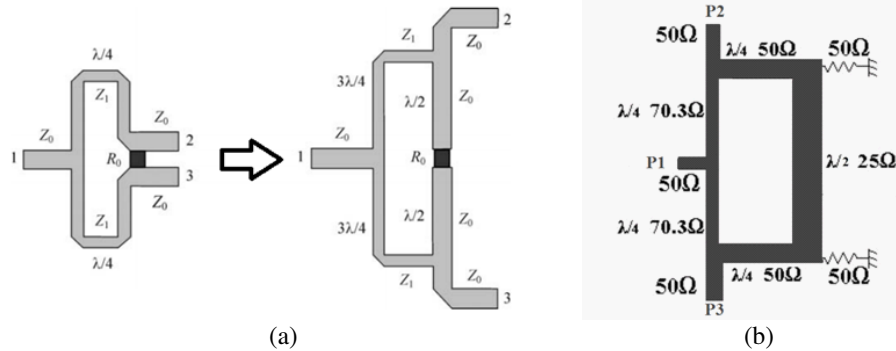


Figure 1. (a) Wilkinson PCD with extra half wavelength [3], (b) original configuration of Gysel combiner.

2. PROPOSED MODEL

The proposed Gysel design provides three additional degrees of freedom compared to standard structures including the value of the load resistor as well as the length and width (or characteristic impedance) of the meandered stepped-impedance load line. At first glance, the addition of an extra load line would imply an increase in the overall device size but, as demonstrated in this work, careful meandering of the additional lines helped make our design more compact without degrading performance. Additional design flexibility to the Gysel structure allows for narrower transmission lines. Microstrip lines with the narrower width not only reduce the size of the Gysel PCD but also make them easier to meander and thus leading to a more compact design in comparison with the original configuration of Gysel PCD. The proposed configuration also shows a wider frequency response with approximately 10% fractional

bandwidth for 20 dB return loss. In contrast, conventional Gysel PCDs have demonstrated fractional bandwidths of 5% or less [2]. This improvement is mainly caused by the high order harmonic rejection properties resulting from the use of stepped impedance line sections.

Figure 2 shows the schematic of the proposed Gysel PCD. In this figure, all characteristic impedances (Z_a , Z_b , Z_c , and Z_d) and load values (R_L) have been respectively normalized to z_a , z_b , z_c , z_d , and r_L , relative to the system impedance of $Z_0 = 50 \Omega$.

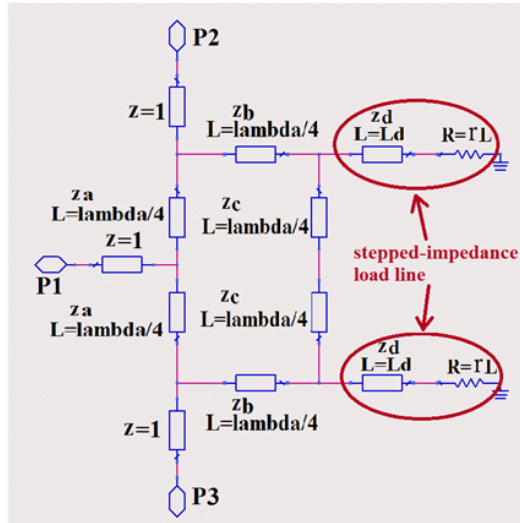


Figure 2. Proposed meandered Gysel with stepped impedance load lines.

Due to symmetry, the configuration of Fig. 2 can be analyzed using the even-odd mode equivalent circuits. The equivalent circuits of even and odd modes of the modified structure and their simplified configurations are shown in Fig. 3.

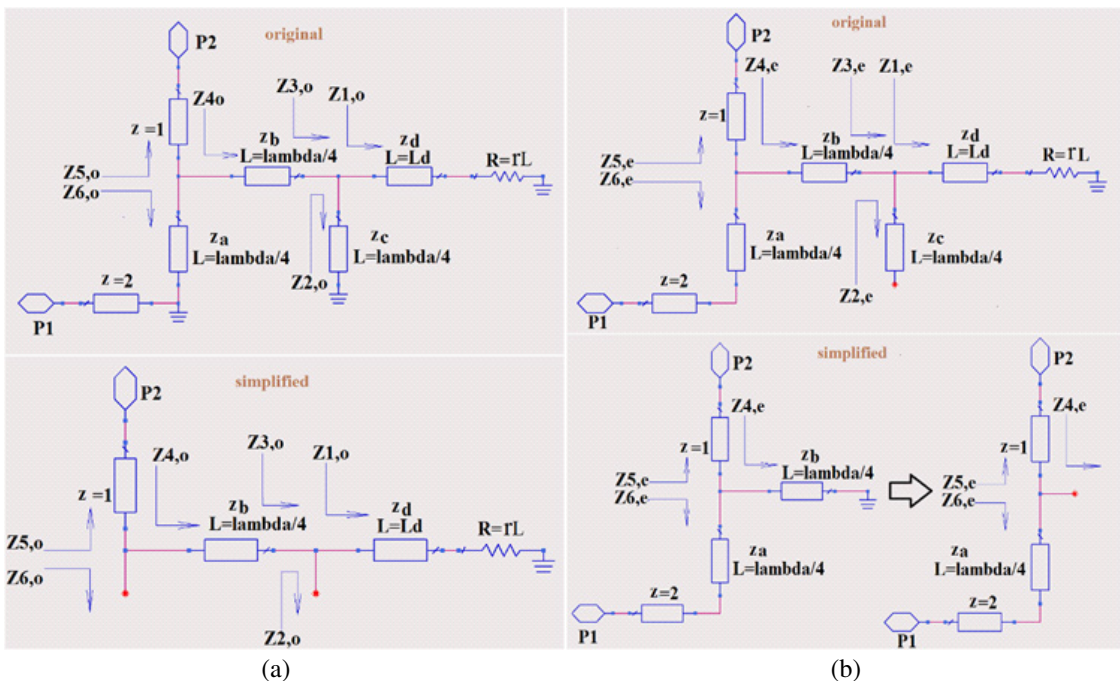


Figure 3. Equivalent circuit and its simplified configuration (a) odd-mode and (b) even-mode.

Due to the narrowband nature of the quarter-wave lines including their non-negligible parasitic effects, low or high impedance terms are used instead of the desired short and open circuits. The seen impedances from different nodes shown in Fig. 3 are reported in Table 2 for both even and odd modes.

Table 2. Seen impedances from the nodes of even & odd mode equivalent circuits.

Input impedance	Even mode	Input impedance	Odd mode
$z_{1,e}$	Any value	$z_{1,o}$	$z_d \frac{r_L + jz_d \tan(\beta L_d)}{z_d + jr_L \tan(\beta L_d)}$
$z_{2,e}$	Short circuit/low impedance	$z_{2,o}$	Open circuit/high impedance
$z_{3,e}$	Short circuit/low impedance	$z_{3,o}$	$z_{1,o}$
$z_{4,e}$	Open circuit/high impedance	$z_{4,o}$	$\frac{(z_b)^2}{z_{3,o}}$
$z_{5,e}$	1	$z_{5,o}$	1
$z_{6,e}$	$z_a^2/2$	$z_{6,o}$	Open circuit/high impedance

Perfect matching between ports 1 and 2 from even mode analysis implies that [17],

$$z_{6,e} = z_{5,e} \Rightarrow z_a = \sqrt{2} \quad (1)$$

while odd mode analysis leads to

$$z_{5,o} = z_{4,o} \Rightarrow z_{3,o} = (z_b)^2 \Rightarrow z_{1,o} = (z_b)^2 \quad (2)$$

As extracted from the even mode analysis, impedance Z_a corresponds to 70.7Ω while any arbitrary value can be chosen initially for Z_b and Z_c . Therefore, to simplify the designing process and reduce the PCDsize, impedance Z_b is set to 70.7Ω ($z_b = \sqrt{2}$) while Z_c is usually set to smaller values in the optimization process to achieve wider bandwidth and higher isolation. Hence

$$z_{1,o} = 2 \quad \text{or} \quad Z_{1,o} = 100 \Omega \quad (3)$$

$$z_d \frac{r_L + jz_d \tan(\beta L_d)}{z_d + jr_L \tan(\beta L_d)} = 2 \quad (4)$$

Optimal values for all other unknown variables z_d , L_d , and r_L , in Eq. (4), can be obtained by using Keysight ADS momentum [16], in which, all the geometrical dimensions are optimized during the simulation process.

Through the algorithm described in Fig. 4, our work also aims to scale and accommodate the proposed improved Gysel PCD for any desirable frequency range. All these steps were closely followed by schematic and layout electromagnetic simulations using ADS Momentum [16] to take into account the high-frequency behavior of all components used. The proposed scalable design flow is described next:

1-Design process is started by solving (4). With its three unknown variables, our first approach is to assume a reasonable value for r_L and then find the smallest applicable length, L_d , and the most

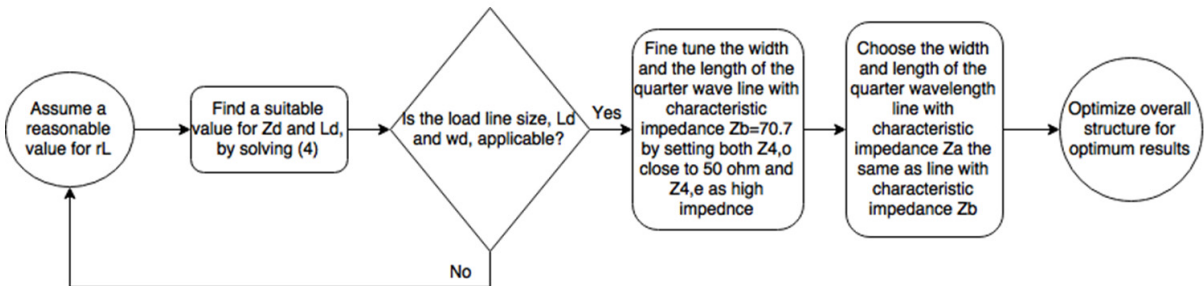


Figure 4. Flowchart of the proposed design process.

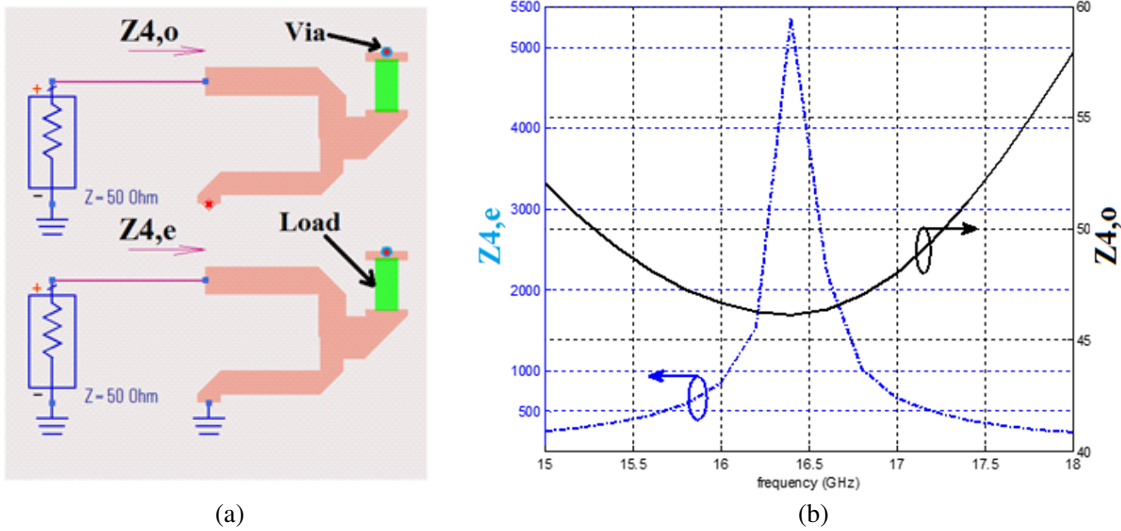


Figure 5. Even-odd mode simulation to determine. (a) schematic view and (b) even and odd mode impedance magnitude.

suitable characteristic impedance, z_d realized with a line width of w_d in order to satisfy (4). Note that, solving (4) or equivalently fitting $Z_{1,o}$ into 5% tolerance of 100Ω , i.e., $[95, 105] \Omega$, for the whole desirable frequency range, is adequate in most practical situations.

2-If the obtained load line size is not suitable, change the load value, r_L , and start again from step 1. In this work, r_L is assumed to be 50Ω for the first two designs while a smaller value is chosen for the last design in order to obtain a practical load line width.

3-The required half wavelength line with characteristic impedance Z_c has no constraints to its width but it should also not be too wide to impede meandering to reduce size. Also, the following conditions must be verified: $z_{3,o} = z_{1,o} = 2$ and $z_{3,e}$ should correspond to low impedance value by tuning the width of Z_c (Fig. 3). Note that for these applications, impedances less than 5Ω can be approximated as low impedances while impedances higher than 1000Ω can be approximated as high impedances.

4-The width and length of the quarter wave line with characteristic impedance $Z_b = 70.7 \Omega$ should be finely tuned by setting both $Z_{4,o}$ close to 50Ω and $Z_{4,e}$ as high impedance (Fig. 3 and Fig. 5).

5-Verify that the width and length of the quarter wavelength line with characteristic impedance Z_a are the same as those of Z_b found in step 4.

6-After connecting and shaping all parts in layout design, the entire structure (Fig. 6(a)) should be optimized and/or fine-tuned to achieve optimum results.

3. SIMULATION AND IMPLEMENTATION

To demonstrate the capabilities of the proposed PCD, three PCDs were implemented and their measured results compared to expected simulated results. Rogers RT-Duroid 5880 substrates were used with a relative permittivity of 2.2 and 0.381 mm thickness to design two PCDs operating at Ku and X bands, while a Rogers TMM10i substrate with a relative permittivity of 9.8 and with 0.381 mm thickness was used to design an X-band Gysel PCD.

3.1. Ku-Band PCD

The first implementation of the modified Gysel PCD was designed to cover the Ku-band using an RT-Duroid 5880 substrate. A center frequency of 16.5 GHz was selected. Fig. 5(a) shows the schematic view used to determine the even and odd modes of Z_4 while Fig. 5(b) shows its momentum co-simulation results.

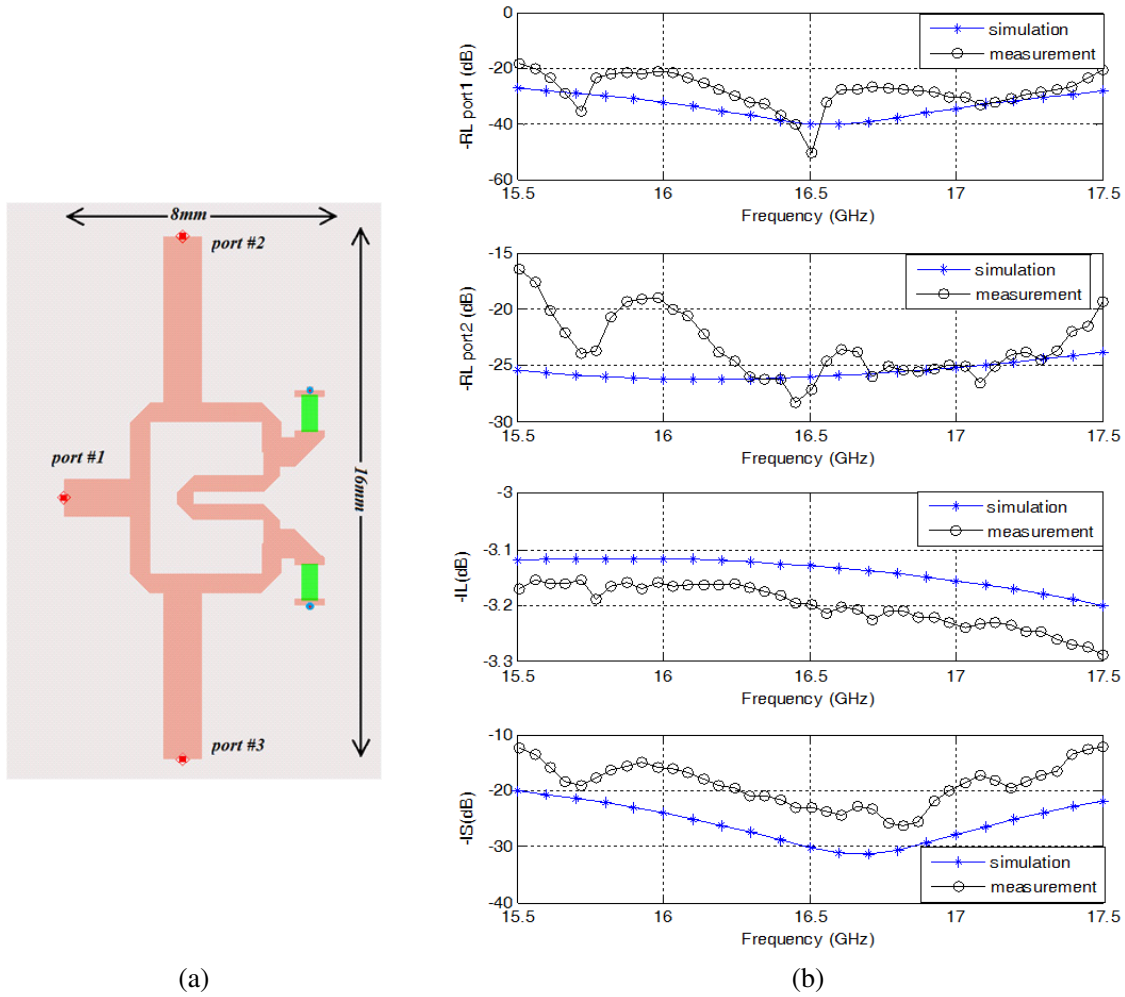


Figure 6. Proposed Ku-band Gysel PCD on RT-Duroid 5880. (a) Layout of meandered Gysel with stepped impedance. (b) Comparison between simulated and measured results.

The complete layout view of the Gysel PCD design is shown in Fig. 6(a). After fabrication, the structure was experimentally validated. The measured results are compared with simulation data in Fig. 6(b) and summarized in Table 3 to further compare them with the referred works reported in Table 1. Performance indicators such as Fractional Bandwidth (FB), Return Loss (RL), Insertion Loss (IL) and Isolation (IS) were used to demonstrate the accuracy and robustness of the designs implemented here.

Figure 7(a) shows an implemented power amplifier module capable of combining four power amplifiers to measure the performance of the proposed Gysel PCD when connected sequentially. Through lines have been used in the place of PAs to measure the exact values of IL and RL of the Gysel PCD without the effects of power amplifiers. The measured S -parameters are shown in Fig. 7(b) indicating a 12% fractional bandwidth with 20 dB return loss or better and operating at a center frequency of 16.5 GHz. The total insertion loss for the overall structure containing four Gysel PCDs was measured to be less than 1 dB, corresponding to 0.25 dB for each of the proposed Gysel PCD.

3.2. X-Band PCDs

Two additional X-band PCD structures were designed, using the proposed algorithm in Fig. 4, and respectively implemented on RT Duroid 5880 ($\epsilon_r = 2.2$) and Rogers TMM10i ($\epsilon_r = 9.8$) substrates, to operate at the center frequency of 9.5 GHz. The selected load resistance (R_L) for designs implemented

Table 3. A summary of measurement achieved results.

Bandwidth for	Ku-band on RT-Duroid5880	X-band on RT-Duroid5880	X-band on TMM10i
< 0.25 dB IL	15.5–17.3	8.7–10.3	0
< 0.5 dB IL	15.5–17.5	8.5–10.5	8.8–10.1
> 20 dB RL	15.5–17.5	8.8–9.8	8.7–9.9
> 15 dB RL	15.5–17.5	8.5–10.5	8.5–10.5
> 15 dB IS	15.9–17.3	8.5–10.5	8.5–10
< 0.1 dB unbalance power between splitting ports	15.5–17.5	8.5–10.5	8.5–10.5

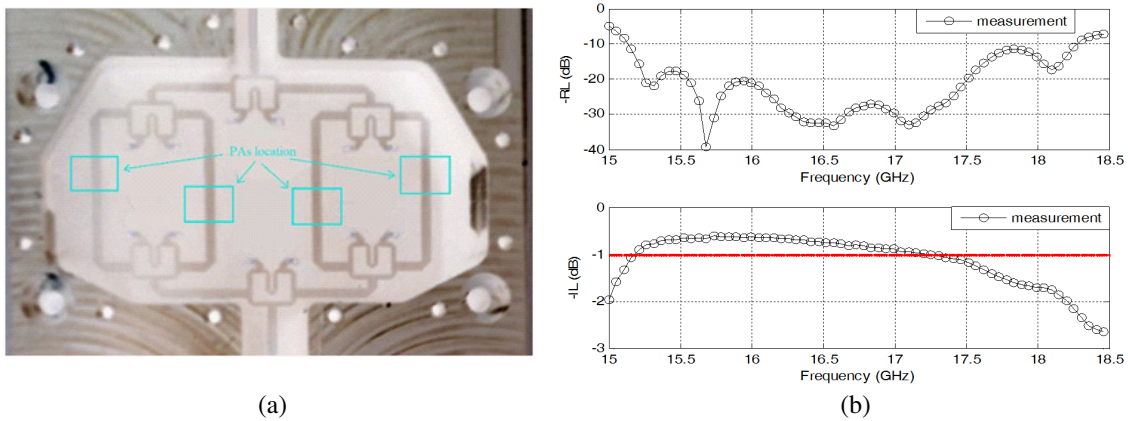


Figure 7. 4-PA combiner Ku-band module on RT-Duroid 5880, (a) photograph, (b) measurement results.

in Rogers 5880 substrates was 50Ω . However, for the design implemented in Rogers TMM10i, this value led to a load line width less than 0.07 mm , which is impractical with available printed circuit board technology. As a result, R_L was recalculated to $Z_{1,o} \cong 100 \Omega$ with a corresponding load impedance of 33Ω . The simulated layout and its fabricated counterpart PCD on RT-Duroid 5880 are shown in Fig. 8(a) while the simulated layout PCD on Rogers TMM10i is shown in Fig. 8(b). Although Rogers TMM10i substrates are more lossy than RT Duroid 5880 substrates, a smaller PCD can be accomplished by using Rogers TMM10i due to its bigger relative permittivity. As displayed in Fig. 8 and Fig. 9, at the expense of increasing the 0.15 dB IL, the size of PCD fabricated on Rogers TMM10i is roughly reduced to 0.25% of the size of PCD implemented on RT Duroid 5880. A comparison between simulation and measurement results for both designed PCDs are shown in Fig. 9 to demonstrate the superior performance of the proposed Gysel PCD approach. The measured results agree with the simulation ones, thus demonstrating the proposed structure and design process. A summary of the measurement results is displayed in Table 3 to compare with the referred works reported in Table 1.

Four PAs can be combined in the way displayed in Fig. 10(a) to create an amplifier module suitable for SSPAs. In this configuration, Wilkinson PCDs were used as dividers because they occupy smaller areas and do not need a high power load resistor. The used Wilkinson PCDs on RT-duroid 5880 exhibits an IL less than 0.15 dB and an RL greater than 25 dB from 8 to 11 GHz . Note that through lines have been again used instead of PAs to measure the total IL of this structure. The measurement results, shown in Fig. 10(b), indicate a fractional bandwidth of 10% at the center frequency of 9.5 GHz and a return loss of about 20 dB , while the insertion loss is less than 0.8 , i.e., less than $\frac{0.8 - 2 \times 0.15}{2} = 0.25 \text{ dB}$ for one proposed Gysel PCD.

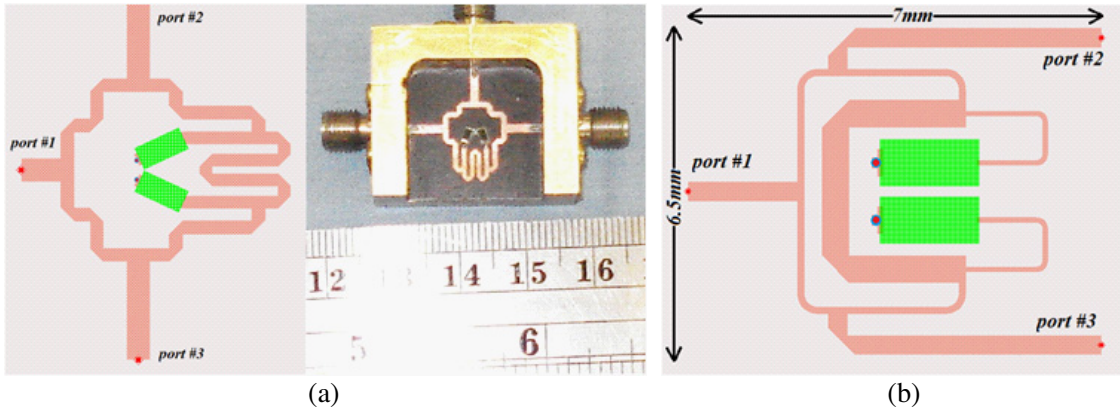


Figure 8. X-band Gysel C/D. (a) Layout and photograph of the designed prototype of meandered Gysel with stepped impedance on RT-Duroid 5880, (b) layout of the designed prototype of meandered Gysel with stepped impedance on TMM10i.

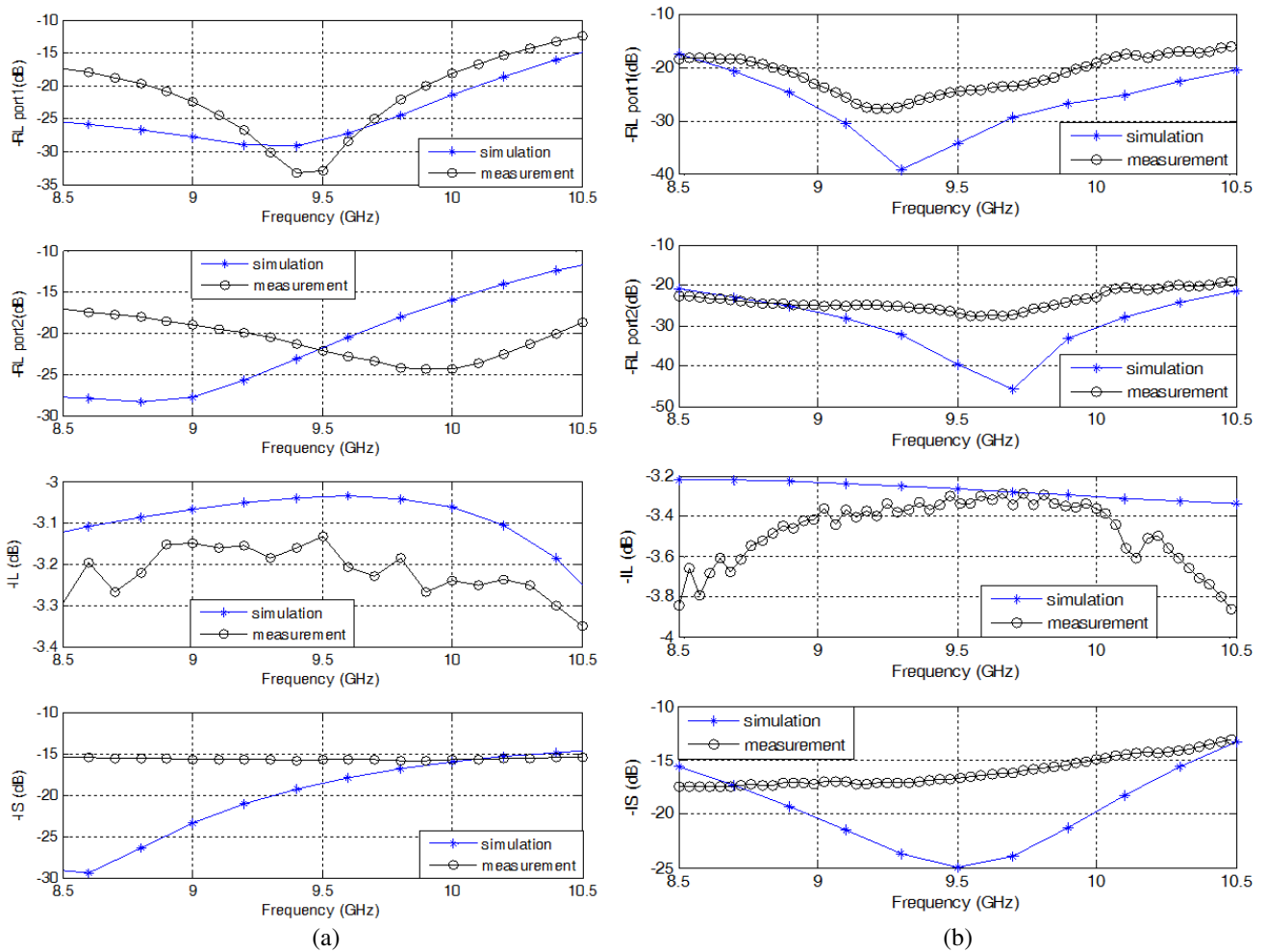


Figure 9. Comparison between simulated and measured results of the proposed X-band Gysel PCD on (a) RT-Duroid 5880 and (b) TMM10i.

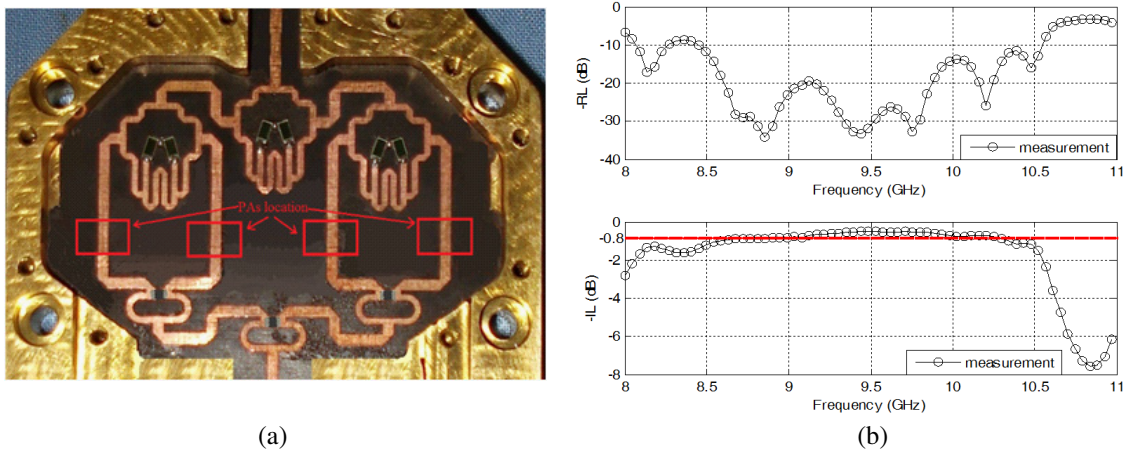


Figure 10. X-band 4-PA combiner module on RT-Duroid 5880 (a) photograph (b) measurement results.

The utilized RF load resistors, in all three implemented PCDs, are terminated to its bottom conductive plate at one of their ends in the manufacturing process. Hence the substrate area underneath of the loads is removed to ground the terminated end as well as making better heat transferring. The load resistors used in X-band can tolerate a power up to 50 W while Ku-band resistors can tolerate up to 20 W.

4. CONCLUSION

This paper presents an enhanced configuration of Gysel combiner/divider using stepped impedance and meandered load lines with design flexibility leading to smaller sizes with superior performance. The analytical analysis is based on the even-odd method while most of the designing steps are performed with the help of a commercial planar electromagnetic simulator. This paper also proposes an optimization algorithm to scale the improved structure to any suitable frequency thus reducing design time. Three separate designs are fabricated and tested, two on RT-Duroid 5880 substrate and the third one on Rogers TMM10i to further demonstrate the accuracy of our proposed algorithm and superior performance of the improved Gysels structure. Overall, measured results are in a good agreement with simulated ones. The fabricated structures demonstrate the superior performance of the proposed approach, with higher return loss (more than 20 dB), much lower insertion loss (less than 0.25 dB) and very negligible amplitude unbalance (less than 0.05% dB) over a sufficiently wide bandwidth (more than 10% fractional bandwidth) making them suitable for high power combiners.

REFERENCES

1. Wilkinson, E. J., "An N-way hybrid power divider," *IRE Trans. Microwave Theory Tech.*, Vol. 8, No. 1, 116–118, Jan. 1960.
2. Walker, J. L. B., *Handbook of RF and Microwave Power Amplifiers*, 542–544, Cambridge University Press, 2012.
3. Grebennikov, A., *RF and Microwave Transmitter Design*, 175–177, John Wiley & Sons, 2011.
4. Kao, J. C., Z. M. Tsai, K. Y. Lin, and H. Wang, "A modified Wilkinson power divider with isolation bandwidth improvement," *IEEE Transactions on Microwave Theory and Techniques*, Vol. 60, No. 9, 2768–2780, 2012.
5. Ahmed, O. and A. R. Sebak, "A modified Wilkinson power divider/combiner for ultrawideband communications," *International Symposium in IEEE Antennas and Propagation Society*, 1–4, 2009.

6. Horst, S., R. Bairavasubramanian, M. M. Tentzeris, and J. Papapolymerou, "Modified Wilkinson power dividers for millimeter-wave integrated circuits," *IEEE Transactions on Microwave Theory and Techniques*, Vol. 55, No. 11, 2439–2446, 2007.
7. Gysel, U. H., "A new N-way power divider/combiner suitable for high-power applications," *IEEE MTT-S Microwave Symp.*, Palo Alto, CA, 1975.
8. Abbosh, A. and B. Henin, "Planar wideband inphase power divider/combiner using modified Gysel structure," *IET Microw. Antennas Propag.*, Vol. 7, No. 10, 783–787, 2013.
9. Xia, B., L. Sh. Wu, and J. Mao, "A new balanced-to-balanced power divider/combiner," *IEEE Transactions on Microwave Theory and Techniques*, Vol. 60, No. 9, 2791–2798, Sept. 2012.
10. Lin, F., Q. X. Chu, Z. Gong, and Z. Lin, "Compact broadband Gysel power divider with arbitrary power-dividing ratio using microstrip/slotline phase inverter," *IEEE Transactions on Microwave Theory and Techniques*, Vol. 60, No. 5, 1226–1234, May 2012.
11. Oraizi, H. and A. R. Sharifi, "Optimum design of a wideband two-way Gysel power divider with source to load impedance matching," *IEEE Transactions on Microwave Theory and Techniques*, Vol. 57, No. 9, 2238–2248, Sept. 2009.
12. Zhang, H., X. Shi, F. Wei, and L. Xu, "Compact wideband Gysel power divider with arbitrary power division based on patch type structure," *Progress In Electromagnetics Research*, Vol. 119, 395–406, 2011.
13. Guan, J., L. Zhang, Z. Sun, Y. Leng, and Y. Peng, "Designing power divider by combining Wilkinson and Gysel structure," *Electronics Lett.*, Vol. 48, No. 13, 769–770, 2012.
14. Zaker, R., A. Abdipour, and R. Mirzavand, "Closed-form design of Gysel power divider with only one isolation resistor," *IEEE Microwave and Wireless Components Letters*, Vol. 24, No. 8, 527–529, 2014.
15. Wu, Y., Y. Liu, and S. Li, "A modified Gysel power divider of arbitrary power ratio and real terminated impedances," *IEEE Microwave and Wireless Components Letters*, Vol. 21, No. 11, 601–603, 2011.
16. Keysight ADS Momentum, v. 2009.
17. Pozar, D. M., *Microwave Engineering*, 4th edition, 328–331, John Wiley & Sons, 2011.